in HFI causes displacement of the brain which in turn strains the pituitary stalk resulting in the various endocrine manifestations of this syndrome (*4*).

The pathogenesis of this condition serves to explain the findings on the labeled leukocyte study. The frontal bones of the skull, along with most of the remainder of the calvarium, are comprised of two layers of compact bone known as the inner and outer tables. These two tables are separated from each other by the diploe, the cancellous bone containing hematopoietically active marrow within its interstices (*5*). The calvarial thickening of HFI is generally confined to the squamous portion of the frontal bones of the skull, and results from new bone deposition by the dura on the inner table. As the dura deposits new bone along the interior border of the inner table, the inner table itself undergoes spongification on its diploic side, resulting in excessive diploic bone in the thickened part of the calvarium (*4*). This increased diploic space is accompanied by a similar increase in the quantity of marrow, and it is this increased volume of marrow that undoubtedly accounts for the increased activity observed on labeled white cell images. The symmetric appearance of such increased calvarial activity is useful for distinguishing HFI from infection (*1,2*). Not all cases of HFI are symmetric, however, as this case illustrates, and in this situation determining the cause of the increased activity, is more problematic. Under these conditions, marrow scintigraphy can provide useful information. If the leukocyte and marrow images are spatially congruent, the findings on the labeled leukocyte study can be attributed to the increased marrow volume associated with HFI; if there is no activity on the marrow images corresponding to that on the leukocyte study, then the findings on the leukocyte study are due to infection (*6,7*).

CONCLUSION

Increased frontal bone activity on labeled leukocyte images of patients with HFI is due to the increased volume of marrow present in this condition; when doubts about the etiology of this increased uptake arise, adjunctive marrow imaging can provide useful information.

REFERENCES

1. Floyd JL, Jackson DE Jr, Carretta R. Appearance of hyperostosis frontalis interna on indium-111-leukocyte scans: potential diagnostic pitfall. *J Nucl Med* 1986;27:495–497.
2. Paulson E, Datz FL. False-positive calvarial uptake of indium-111 leukocytes in a patient with hyperostosis frontalis interna. *Clin Nucl Med* 1988;13:68–69.
3. Thakur ML, Lavender JP, Arnot RN, Silvester DJ, Segal AW. Indium-111-labeled autologous leukocytes in man. *J Nucl Med* 1977;18:1014–1021.
4. Various Hyperostoses of Obscure Origin. In: Jaffe HL, ed. *Metabolic, degenerative and inflammatory diseases of bones and joints*. Philadelphia: Lea and Febiger; 1972:272–300.
5. Osteology. In: Warwick R, Williams PL, eds. *Grays anatomy*, 35th ed., Edinburg, Longman; 1973:200–387.
6. Palestro CJ, Kim CK, Swyer AJ, Capozzi JD, Solomon RW, Goldsmith SJ. Total hip arthroplasty: periprosthetic ^{111}In-labeled leukocyte activity and complementary ^{99m}Tc sulfur colloid imaging in suspected infection. *J Nucl Med* 1990;31:1950–1955.
7. Palestro CJ, Roumanas P, Kim CK, Goldsmith SJ. Diagnosis of musculoskeletal infection using combined ^{111}In-labeled leukocyte and ^{99m}Tc-sulfur colloid marrow imaging. *Clin Nucl Med* 1992;17:269–273.

Compartmental Analysis of the Complete Dynamic Scan Data for Scintigraphic Determination of Effective Renal Plasma Flow

M.S. Dagli, V.J. Caride, S. Carpenter and I.G. Zubal

Division of Imaging Science, Department of Diagnostic Radiology, Yale Medical School, New Haven, Connecticut; and Section of Nuclear Medicine, Department of Radiology, The Hospital of Saint Raphael, New Haven, Connecticut

We have developed an image-based compartmental analysis for estimating effective renal plasma flow (ERPF in units of milliliters per minute) from the full time-activity curves of regions of interest (ROI) placed over the heart, kidneys and bladder. **Methods:** Kidney or time-activity curves are corrected for physical attenuation using estimates of kidney depth derived from patient height and weight. Estimates of the calibration factors, K_p and K_b (mCi/counts/sec), for the plasma and bladder time-activity curves are determined by applying the following ROI analysis to each frame of the dynamic scan: $(K_p)P_c(t) + (K_b)B_c(t) = D_i - R_q(t)$, where $P_c(t)$ and $B_c(t)$ represent the counting rates measured in ROI placed over the left ventricle blood pool and bladder at time t; D_i is the known total injected dose, and $R_q(t)$ represents the millicurie of tracer in the kidneys at time t. Once K_p and K_b have been determined by regression, the calibrated time activity curves are used to solve for the physiological parameter fERPF (min^{-1}), which represents the fraction of the total body plasma cleared of mertiatide per min. The ERPF calculated by the product of fERPF and plasma volume, determined from patient weight, was compared to the ERPF as calculated by blood samples and the Schlegel and renal uptake plasma volume product scintigraphic techniques. **Results:** Twenty-five adult patients with a wide range of ages and renal function were studied. The results of this image-based method for calculating ERPF correlated well with the values obtained from blood samples (linear regression slope = 1.06; y-int = −34.68 ml/min, r = 0.905) and offered a significant improvement over both the Schlegel and renal uptake plasma volume product estimates ($p < 0.05$). **Conclusion:** A scintigraphic estimation of ERPF without blood samples using time-activity data from the heart, kidneys and bladder acquired over the entire renogram is feasible and correlates well with more invasive techniques requiring blood samples.

Key Words: renal scintigraphy; technetium-99m-mertiatide; effective renal plasma flow; compartmental model

J Nucl Med 1997; 38:1285–1290

The accurate purely scintigraphic estimation of renal function has long been a goal in clinical nuclear medicine. Current clinically useful measurements of effective renal plasma flow (ERPF) require one or two blood samples for the processing of

Received Mar. 22, 1996; revision accepted Oct. 8, 1996.

For correspondence or reprints contact: George Zubal, PhD, Yale University School of Medicine, P.O. Box 208042, New Haven, CT 06520-8042.

cardiac and renal time-activity curves or for use in regression equations (*1*). A computer model based procedure could potentially standardize the analysis and allow the calculation to become a routine adjunct to the renogram by obviating invasive blood sampling.

Several camera-only methods have been developed that rely only on the total renal uptake (RU) during the purely parechymatous phase of the renogram, i.e., before tracer excretion into the bladder (*2–4*). These methods produce results that are reasonable but which have room for improvement, in part due to: (a) the short time interval used for obtaining crucial data, (b) sensitivity to errors in kidney depth estimates, (c) variations in kidney excretion times and (d) the need to assume a constant tracer concentration in the plasma during the time used for analysis. These factors limit the ultimate potential accuracy of any technique using this type of approach. Because of this, it seems reasonable that a method based on the time-activity curves of the plasma, kidneys and bladder, produced over the entire renogram, would yield a more robust estimation of clearance.

We have approached this task by applying the techniques of compartmental analysis and modeling the biokinetics of ^{99m}Tc-MAG_3 in the body as a three compartment system: plasma, kidneys and bladder. Through this method we are able to calculate the fraction of the plasma volume that is cleared by the kidneys each minute (fERPF with the units of min^{-1}). This parameter is independent of patient size and can be used for interpatient comparison (*5*). If necessary, fERPF may be multiplied by an estimate of plasma volume to be transformed into the absolute physiological parameter, ERPF (ml/min).

MATERIALS AND METHODS

Subjects

The population studied consisted of 25 patients referred to nuclear medicine for the evaluation of renovascular disease. There were 11 males and 14 females (average weight 78.9 ± 19.2 kg, average height 167.1 ± 8.9 cm, average age 62.9 ± 12.6 yr), with MAG_3 plasma clearances ranging from 64–611 ml/min. Patients were excluded when blood samples were not obtained or when the heart and bladder were not included in the field of view. No other selection criteria were applied.

Data Acquisition

All patients were studied using the routine renogram protocol at the institution, which called for the sequential injections of ^{99m}Tc-DTPA and ^{99m}Tc-MAG_3 to calculate both glomerular filtration rate (GFR) and ERPF (*6*). Only data collected from the MAG_3 portion of the study were used for this analysis. The patients were imaged supine with the gamma camera positioned underneath the imaging table. After oral hydration, approximately 1 mCi (1 mCi = 37 Mbq) of ^{99m}Tc-DTPA was injected in an antecubital vein as the acquisition program was activated. Six minutes later, a diuretic (furosemide 0.5 mg/kg) was injected and followed at 7 min by approximately 10 mCi of ^{99m}Tc-MAG_3 (Mallinkrodt, ^{99m}Tc-mertiatide). The use of a diuretic assured a more complete removal of tracer activity from the renal pelvis without affecting the renal plasma flow (*7*). This protocol has been shown to have little effect on methods that base MAG_3 clearance estimates on the RU of tracer at 2 min (described later) (*2,6*). Because the observed DTPA radioactivity in the bladder and plasma just before the MAG_3 injection was negligible relative to the eventual observed radioactivity of the MAG_3, it was concluded that the DTPA on board would have a minimal effect on the complete dynamic scan ERPF analysis as well. In an ideal situation, however, the protocol would call for only the administration of MAG_3

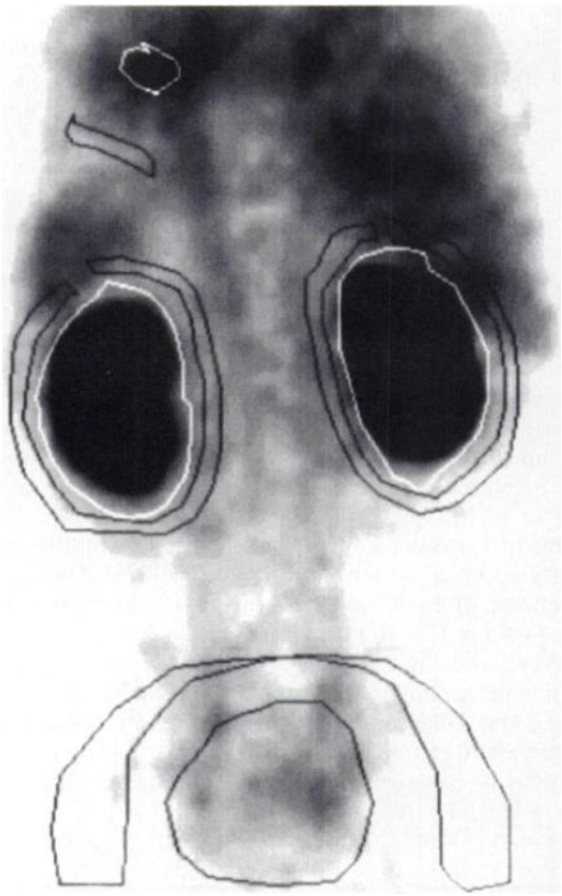

FIGURE 1. Computer display showing ROI for the heart, kidneys and bladder and the areas used for background correction.

The studies were done with a camera with a UFOV of 40 × 20 cm and a matrix of 64 × 64 pixels (Trionix XLT 20 System; Trionix Research Laboratory, Inc., Twinsburg, OH). The 40-cm axis was aligned with the long axis of the subject so that a complete view of the heart, kidneys and bladder could be obtained. The dynamic data were collected at a rate of one frame every 15 sec for approximately 30 min. The sensitivity of the camera (counts/sec/mCi) was determined before each study by imaging 1 mCi of ^{99m}Tc placed at 30 cm from the center of the detector. The camera was calibrated by this method each day with camera settings the same as those used for the patient acquisitions.

Regions of interest (ROI) were drawn for the kidneys, bladder and left ventricle as shown in Figure 1. The kidney signals were calibrated using an approximately 2 pixel wide concentric background ROI surrounding each organ. The bladder was similarly background corrected with a large semicircular ROI surrounding it. This background region was narrowed at the top of the bladder to avoid contamination by activity from the ureters. To correct the cardiac signal for contamination from the extravascular space, background subtraction was done using a thin rectangular shaped ROI on the left lung in the space between the heart and the spleen (*8*).

The ERPF (ml/min) was determined for each patient using a two blood sample clearance technique (*4*). Two 10-cc blood samples were obtained from an antecubital vein contralateral to the side of radiotracer injection, at 20 and 60 min after the ^{99m}Tc-MAG_3 injection. After centrifugation for 5 min at 1310 g, duplicate 1-cc samples were counted in a well counter (1282 Compugamma, Pharmacia LKB Nuclear Inc.). The total injected activity (TID) was determined from an aliquot of the ^{99m}Tc-MAG_3 preparation

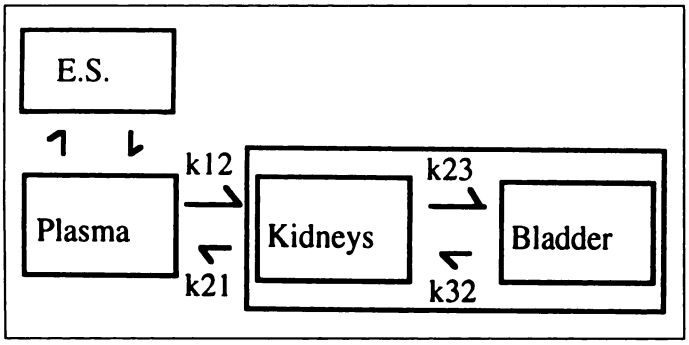

FIGURE 2. Four-compartment model describing the distribution of most injected tracers. For ^{99m}Tc-MAG_3, k21 and k32 are negligible, and diffusion into the extravascular space is slow. Thus, a three-compartment model can be used if this tracer movement is considered negligible. In the two-compartment model, the renal and bladder compartments are combined as one.

used for the study corrected for a dilution factor. The plasma activity at time zero (A_0) was obtained by back extrapolation and the rate of disappearance (k) was computed from the logarithmic slope. The ERPF (ml/min) was calculated by the formula:

$$ERPF = [TID/A_0]k. \quad \text{Eq. 1}$$

For comparison to previously published scintigraphic techniques, the ERPF was also estimated by the Schlegel and the RU plasma volume product (RUPV) method using the first 2 min of MAG_3 uptake data generated from the renal regions of interest (*2–4*). The RUPV method estimates MAG_3 clearance (ml/min) to be the product of the fraction of the injected dose present in the kidneys at 2 min and an estimate of plasma volume. The Schlegel method calculates MAG_3 clearance by substituting the RU at 2 min into a regression equation based on a precollected database.

Data Analysis

The complete distribution of MAG_3 over time can be modeled with the four compartment system shown in Figure 2, consisting of the blood plasma, kidneys, bladder and the extravascular space (*9*). In this system the material is exchanged between compartments at a rate proportional to the quantity remaining in each compartment (*10*).

This system can be simplified to either a three or two compartment model. Because there is minimal reflux of tracer from the kidney to the blood and the bladder to the kidney, k21 and k32 are effectively zero. If the transfer of radiotracer to the extravascular space is considered to be negligible, the system is reduced to three compartments: the plasma, the kidneys and the bladder. In this study, the three compartment model is used in the calibration of the time-activity curves of the plasma and bladder so that they represent the amount of tracer in millicuries present in the compartments over time. The two physiologically relevant kinetic parameters, k12 and k23, represent, respectively, the fractional effective renal plasma flow (fERPF in units of min^{-1}) and the fractional excretion rate of the kidney to the bladder per minute.

In the two compartment model, the kidneys and bladder are combined as one kidney + bladder compartment; thus, the model is left with only one kinetic parameter, fERPF (k12). In this study, the two compartment model is used in the final estimation of fERPF using the calibrated time-activity curves of the plasma, kidneys and bladder. When fERPF is multiplied by the patient's plasma volume, an estimate of ERPF is obtained with the units of milliliters per minute.

Calibration of Plasma and Bladder Curves

The determination of fERPF (k12) through kinetic analysis requires the knowledge of the radioactivity (mCi) present in each of the compartments over time. Therefore, the detected counts should be corrected for tissue attenuation. The availability of regression equations to estimate kidney depth allows correction of the renal time-activity curve by dividing the background corrected renal counts by an attenuation factor $e^{-\mu x}$, where x is the estimated kidney depth, and μ is the γ attenuation coefficient through soft tissue (0.12 cm−1) (*11*). Although no similar equations are available to calibrate the bladder and cardiac activity curves, use of the three compartment model of MAG_3 distribution allows for the calculation of these calibration factors through least-squares regression.

If it is assumed that the volume of distribution of the tracer during the time period of the renogram consists solely of the plasma, kidneys and bladder, then the sum of tracer quantity in each of these three compartments is equal to the injected dose.

$$P_q + R_q + B_q = D_i. \quad \text{Eq. 2}$$

To calibrate the plasma time-activity curve (P_c) so that it reflects the actual millicurie amount of tracer present in the plasma, it must be multiplied by a tissue attenuation correction factor, by a plasma proportion constant that reflects the ratio of the volume of plasma in the cardiac ROI to the total plasma volume and by a camera sensitivity constant that is equal to 1/(camera sensitivity). These three constants can be lumped together into a single plasma calibration factor, K_p (mCi/count/sec). Similarly, so that it reflects the actual millicurie amount of tracer present in the bladder, the bladder time-activity curve (B_c) must be multiplied by an attenuation correction factor and the camera sensitivity constant, the two of which can be lumped together as K_b (mCi/count/sec). Thus, Equation 2 can be rewritten as:

$$(P_c)(K_p) + (B_c)(K_b) = Di - R_q. \quad \text{Eq. 3}$$

If the background corrected values of P_c, B_c and R_q obtained from each 15-sec acquisition of the renogram are applied to the above equation, the following system of simultaneous equations overdetermine the solution for K_p and K_b. In this study, the first min of MAG_3 data was not used in order to allow time for bolus mixing in the circulation.

$$\begin{bmatrix} P_{c5} & B_{c5} \\ P_{c6} & B_{c6} \\ \cdot & \cdot \\ \cdot & \cdot \\ P_{c92} & B_{c92} \end{bmatrix} \times \begin{bmatrix} Kp \\ Kb \end{bmatrix} = \begin{bmatrix} D - R_{q5} \\ D - R_{q6} \\ \cdot \\ \cdot \\ D - R_{q92} \end{bmatrix}. \quad \text{Eq. 4}$$

This system can then be transferred to any standard statistical package such as StatWorks (Cricket Software Inc., Philadelphia, PA) and be solved by multiple linear regression. Once the K_p and K_b parameters have been found, they are multiplied with the plasma and bladder time-activity curves to produce time-quantity curves.

Determination of fERPF (k12) and ERPF

Using the calibrated time-activity curves, the fractional effective renal plasma flow (k12) can be determined through kinetic analysis using either the two or three compartment models. When fERPF is the only parameter desired, the former model is preferred because of its simplicity and fewer degrees of freedom. In this model, the first derivative of the quantity of tracer in each compartment with respect to time is given by the following system of differential equations, where Q_1 and Q_2 represent the quantity of MAG_3 in the plasma and kidney-bladder compartments, respectively:

$$\frac{dQ_1}{dt} = -k_{12}(Q_1) \qquad \frac{dQ_2}{dt} = k_{12}(Q_1) \quad \text{Eq. 5}$$

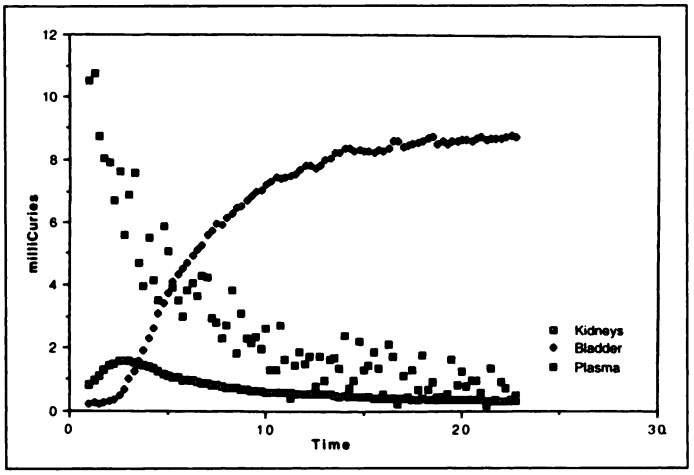

FIGURE 3. Calibrated time-activity curves showing the amount of tracer (mCi) in the plasma, kidneys and bladder.

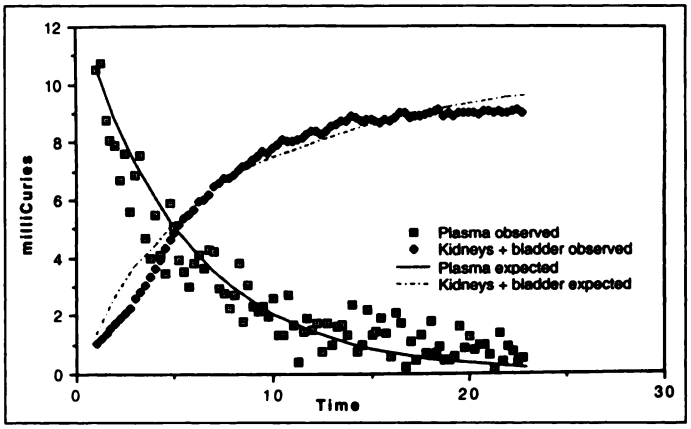

FIGURE 4. Overlay graph of the observed calibrated plasma and kidney + bladder time-activity curves with the expected curves given the two compartment model and the optimized fERPF parameter.

which when solved produces a mathematical description of the amount of tracer in each of the compartments over time in terms of k12 and time (t). The constant, c, is dependent on the injected dose of the tracer.

$$Q_1(t) = ce^{-k_{12}t} \qquad Q_2(t) = c(1 - e^{-k_{12}t}). \qquad \text{Eq. 6}$$

To estimate the parameter k12, a two compartment modeling program originally designed for use with FDG data was used. By toggling on/off the program's parameters it was possible to fit the software to the MAG_3 model. This program accepted as input the calibrated plasma time-activity curve and the sum of the calibrated kidney and bladder time-activity curves and then optimized for fERPF (k12) using the Levenberg–Marquardt algorithm (*12*).

To convert fERPF into an absolute measurement of renal function with the units of milliliters per minute it can be multiplied by an estimate of plasma volume provided by the following relationship (*13*):

$$PV = 84.5\ W^{0.80635} \qquad \text{Eq. 7}$$

where PV is an estimate of the total plasma volume in milliliters, and W is the body weight in kilograms.

To estimate the sensitivity of the three scintigraphic methods to errors in the estimation of kidney depth, the percent change in ERPF was determined in 10 patients after increasing the calculated kidney depth by 1.02 cm. The 1.02 cm increment is the s.e. of the equations used to estimate kidney depth (*11*).

Statistics

To evaluate the improvement in the ERPF estimates of the complete dynamic scan analysis over those of the Schlegel and RUPV methods, the mean squared errors of the regression lines were compared using an f-test. Average kidney depth sensitivity values were compared using an unpaired Student's t-test. Statistical significance was defined as $p < 0.05$.

RESULTS

The average values for the plasma (k_p) and bladder (k_b) calibration factors were 0.235 mCi/count/sec (range: 0.113–0.633) and 0.00999 mCi/count/sec (range: 0.00330–0.0248). The average standard errors of estimate in the determination of these constants by the regression software were ±3.1% and ±2.9%, respectively. This is a measure of the identifiability of the parameters by the regression process and should not be confused with the s.d. of the parameters in the population. Figure 3 shows an example of the plasma, kidney and bladder time-quantity curves produced by the product of each time-activity curve with its respective calibration constant.

Figure 4 shows the overlay of the observed plasma and kidney + bladder calibrated curves for a typical subject with those expected given the two compartment model and the optimized value of fERPF. The average fERPF (k12) value for the 25 subjects was 0.095 (min^{-1}, range: 0.0327–0.184) with an average s.e. of ±4%. A graph of fERPF versus blood ERPF is shown in Figure 5. A correlation coefficient of r = 0.855 indicates a strong linear relationship between the two. The y-value of 3143.7 ml when fERPF is one represents the average volume from which the kidneys are extracting the tracer. This is well within the range of plasma volume.

Figure 6 shows the ERPF calculated by the product of fERPF and plasma volume plotted against the reference ERPF obtained with the two blood samples technique (regression line: y = 1.06x − 34.68; r = 0.905; s.e.e. = 64.1 ml/min). Plasma volume estimates for all patients were obtained by using Equation 7.

Figures 7 and 8 show the ERPF calculated with the Schlegel technique and the RUPV method compared with the reference ERPF. The regression lines are y = 0.71x + 14.22; r = 0.79 and y = 1.09x + 20.29; r = 0.804, respectively, with standard errors of 94.3 ml/min and 91.5 ml/min, respectively.

Comparison of the results from the three scintigraphic methods showed the ERPF estimates of the complete dynamic scan analysis to be better indicators of MAG_3 clearance than those of the Schlegel and RUPV techniques ($p < 0.05$).

In the 10 studies reanalyzed for the evaluation of the error

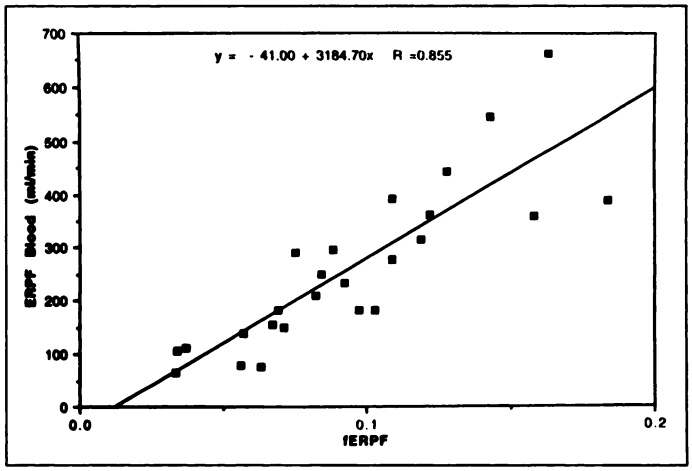

FIGURE 5. Comparison for 25 patients of the reference blood sample ERPF with the fERPF parameter. fERPF represents ERPF divided by plasma volume and was determined from the calibrated time-activity curves.

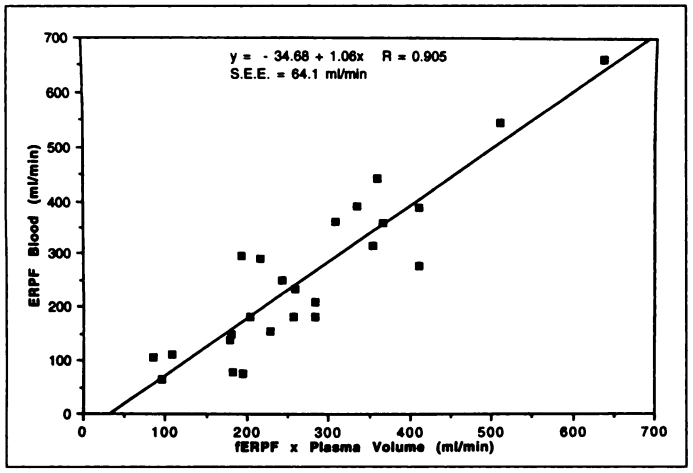

FIGURE 6. Comparison of the reference blood sample ERPF with the results obtained by the complete dynamic scan analysis, which determines ERPF by the product of the fERPF and an estimate of the plasma volume.

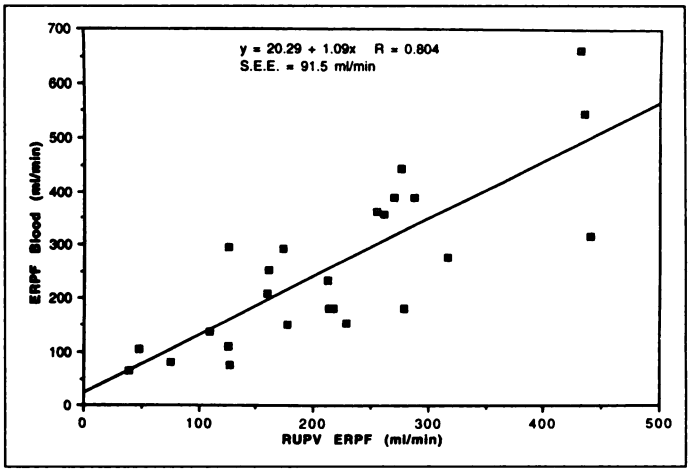

FIGURE 8. Comparison of the reference blood sample ERPF with the results obtained using the scintigraphic RUPV technique, which determines ERPF by the product of the 2-min RU fraction and plasma volume.

introduced by a 1.02 cm overestimation of kidney depth, the Schlegel and RUPV methods had average ERPF increases of 29% and 12%, respectively. In contrast, for the ERPF estimated by the complete dynamic scan method, a significantly lower increase of 2.6% was observed ($p < 0.001$).

DISCUSSION

The current trend towards gamma cameras with large fields of view has made simultaneous kinetic imaging of the heart, kidneys and bladder clinically feasible. We have shown that a compartmental analysis of the distribution of MAG_3 provides an estimate of fERPF (min^{-1}), which represents the fraction of the total body plasma cleared of the tracer by the kidneys each min. fERPF and the rate of RU obtained in the initial 2 min of the renogram when applying the RUPV technique are both measurements of the same parameter and thus have similar values for each subject.

However, by analyzing the time-activity data of every compartment over the entire acquisition time for the fERPF estimation, this method offers several advantages over other techniques. First, it is relatively insensitive to errors in kidney depth. The s.e. of the kidney depth equations is 1.02 cm, or approximately 14%, considering an average kidney depth of 7 cm (*11*). Whereas with the Schlegel and RUPV methods, a 1.02-cm increase in kidney depth resulted in average fERPF increases of 12% and 29%, respectively; with this technique the increase was only 2.6% ($p < 0.001$). Second, this method obviates the need to assume a constant plasma tracer concentration during the portion of the renogram used for analysis. Since the renal extraction of tracer is measured relative to the amount of tracer present in the plasma at each given time, fERPF represents a fraction of the constant volume of plasma being cleared of tracer as it flows through the kidneys and not of the volume defined by the disappearance of tracer from circulation. This concept is substantiated by the plot of fERPF against the reference ERPF (calculated from blood samples), which estimates the volume of distribution as 3143.7 ml, well within the expected range of plasma volume. For the subjects studied, the average plasma volume estimated from body weight was 2944.1 ± 128.7 ml. Finally, by extending the time of measurement from the 2 min used by the Schlegel and RUPV methods to 22 min, a better, time-averaged measurement of fERPF is obtained.

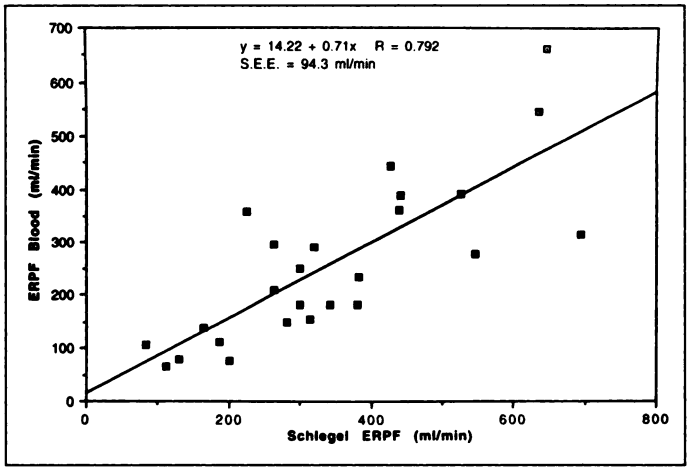

FIGURE 7. Comparison of the reference blood sample ERPF with the results obtained using the scintigraphic Schlegel technique, which determines ERPF by substituting the RU at 2 min into a regression equation based on a precollected database.

The tracer lost to extravascular compartments and extracted by organs other than the kidneys, in particular the liver in the case of MAG_3, will affect the accuracy of the fERPF estimates by causing an overestimation of the calibration factors for the cardiac and bladder time-activity curves. However, the small standard errors of the cardiac and bladder curve calibration factors (±3.1% and ± 2.9%, respectively) support the initial assumption that the distribution of MAG_3 is limited largely to the plasma, kidneys and bladder. This is consistent with the estimated 90% plasma protein binding rate of MAG_3, which restricts its movement into the extravascular space (*14,15*). Because ^{99m}Tc-DTPA, the tracer commonly used to determine GFR, has a significant extravascular diffusion rate, it is uncertain whether this method can accurately estimate GFR. However, when performing dual GFR, ERPF renograms, the calibration factors obtained for the MAG_3 time-activity curves may also be used to calibrate the DTPA curves (*6*). It is also possible that the accuracy of the calibration factors can be improved by varying the time range used for the estimate, or including a term estimating the changing quantity of extravascular tracer over time on the right side of Equation 4. Further studies, however, will be needed to confirm these assumptions.

For comparison to an independent blood standard, it was necessary to convert fERPF (min^{-1}) to the absolute units of milliliters per minute by multiplying it by an estimate of plasma volume, based on patient weight (*13*). This estimate carries its own inherent error that limits the potential accuracy of the absolute ERPF estimate. This problem will be faced by any

scintigraphic technique and makes it difficult to discern improvements in fERPF estimation. Despite this, the complete dynamic scan analysis had a higher correlation with the plasma sample calculation of ERPF ($r = 0.905$) than both the Schlegel ($r = 0.79$) and RUPV ($r = 0.804$) techniques ($p < 0.05$).

CONCLUSION

We have shown that a complete analysis of the dynamic scan data is feasible and provides an accurate estimate of fERPF and ERPF. The method compares favorably with other scintigraphic techniques and is minimally affected by variations in kidney depths, excretion times and plasma tracer concentrations. Because multiplying by an uncertain estimate of plasma volume limits the ultimate potential accuracy of any scintigraphic approach, we suggest that the results be left in their fractional form, fERPF, which would represent ERPF divided by patient plasma volume. In addition to having a distinct technical advantage, this form of ERPF divided by a body fluid volume has also been argued by several authors as having greater physiological value (*5,15*). fERPF already takes into account patient size and thus would not require the traditional clinical procedure of normalization to body surface area (*16*).

REFERENCES

1. Mulligan J, Blue P, Hasbargen J. Methods for measuring GFR with technetium-99m-DTPA: an analysis of several common methods. *J Nucl Med* 1990;31:1211–1219.
2. Caride VJ, Zubal IG, Carpenter S. The rate of renal uptake (RU)–plasma volume (PV) product to estimate the clearance of Tc-99m MAG_3. *J Nucl Med* 1994;35:99P.
3. Schlegel JU, Hamway SA. Individual renal plasma flow determination in 2 min. *J Urol* 1976;116:282–285.
4. Zubal IG, Caride V. The technetium-99m-DTPA renal uptake-plasma volume product: a quantitative estimation of glomerular filtration rate. *J Nucl Med* 1992;33:1712–1716.
5. Peters AM, Allison H, Ussov WY. Measurement of the ratio of glomerular filtration rate to plasma volume from the technetium-99 diethylene triamine pentacetic acid renogram: comparison with glomerular filtration rate in relation to extracellular fluid volume. *Eur J Nucl Med* 1994;21:322–327.
6. Carpenter S, Caride V. Routine renal scintigraphy with sequential injection of technetium-99m-DTPA and technetium-99m-MAG_3. *J Nucl Med Technol* 1994;18: 213–217.
7. Goodman LS, Gilman A, eds. Drugs affecting renal function and electrolyte metabolism. In: *The Pharmacological Basis of Therapeutics, Section VIII.* New York: Macmillan Publishing Co. Inc; 1975.
8. Bell S, Peters AM. Extravascular chest wall technetium-99m diethylene triamine pentaacetic acid: implications for the measurement of renal function during renography. *Eur J Nucl Med* 1991;18:87–90.
9. Sapirstein IA, Vidt DG, Mandel MJ. Volumes of distribution and clearances of intravenously injected creatinine in the dog. *Am J Physiol* 1955;181:330–336.
10. Jacquez J. *Compartmental analysis in biology and medicine.* Ann Arbor, Michigan; University of Michigan Press; 1985.
11. Taylor A, Lewis C, Giacometti A, Hall EC, Barefield KP. Improved formulas for renal depth. *J Nucl Med* 1993;34:1764–1769.
12. Graham MM. Parameter optimization programs for positron emission tomography data analysis. *J Nucl Med* 1992;33:1069.
13. Cropp GJA. Changes in blood and plasma volumes during growth. *J Pediatr* 1971;78:220–229.
14. Eshima D, Taylor A. Technetium-99m mercaptoacetyltriglycine: update on the new T99m renal tubular function agent. *Semin Nucl Med* 1992;2:61–73.
15. Peters AM. Quantification of renal hemodynamics with radionuclides. *Eur J Nucl Med* 1991;18:274–286.
16. White AJ, Strydom WJ. Normalization of glomerular filtration rate measurements. *Eur J Nucl Med* 1991;18:385–390.

Single-Sample Methods to Measure GFR with Technetium-99m-DTPA

Yi Li, Hyo-Bok Lee and M. Donald Blaufox

Department of Nuclear Medicine, The Albert Einstein College of Medicine, Montefiore Medical Center, Bronx, New York

Many single-sample methods have been suggested to simplify the methodology of glomerular filtration rate (GFR) measurement. The relative accuracy of these competing methods is still not clear for clinical practice. **Methods:** Fifty-four GFR studies with ^{99m}Tc-DTPA were performed on 37 adult patients (serum creatinine 0.8–10 mg/dl). Each study included a UV/P, plasma clearance method (three-sample) and single-sample methods. The single-sample methods used were those of Christensen and Groth (modified by Watson), Constable, Dakubu, Groth and Aasted, Jacobsson, Morgan, Russell and Tauxe. **Results:** When the GFR ≥ 30 ml/min ($n = 26$), all of the single-sample methods were highly correlated with UV/P. The correlation of the single-sample method with the plasma clearance was higher than with UV/P. In this group (GFR ≥ 30 ml/min), the Groth 4-hr sample method had the best value of both absolute difference and percent absolute difference (mean ± s.e. = 11.05 ± 2.51 ml/min and 14.08% ± 2.43%, respectively). Most single-sample methods do not perform well at GFR < 30 ml/min ($n = 28$), and none of them has a good correlation with UV/P or plasma clearance at this level of renal function. However, the Groth and Aasted's 4-hr sample method was the best compared with others (mean ± s.e. = 8.43 ± 1.30 ml/min for absolute difference, and 65.91% ± 16.70% for percent absolute difference). **Conclusion:** Single-sample methods may not correctly predict GFR in advanced renal failure. Groth and Aasted's method with 4-hr plasma sample has both the lowest mean absolute difference and percent absolute difference in both the group with GFR ≥ 30 ml/min and GFR < 30 ml/min. All methods perform acceptably at GFR ≥ 30 ml/min.

Key Words: glomerular filtration rate; technetium-99m-DTPA; plasma clearance; urinary clearance; single-sample method

J Nucl Med 1997; 38:1290–1295

Glomerular filtration rate (GFR) can be calculated from the rate of urinary excretion of a constantly infused tracer (classical method) or from the rate of tracer clearance from the plasma after a single intravenous injection. The classic GFR calculation requires blood sampling and often catheterization of the bladder. Clearance also can be calculated using a two-compartment model with multiple blood samples. Classical and multiple blood sample methods for GFR are tedious and time consuming. The single-blood sample method to measure renal function was suggested as early as 1963 by Blaufox (*1*). Since then, one-sample methods were introduced in human study (*2,3*), and there are now a variety of single blood sample methods available. Some investigators used empirical methods comparing the theoretical volume of distribution (V_t) several hours after injection (V_t = dose/plasma activity) with a regression equation (*3–5*). Dakubu (*6*) and Groth and Aasted (*7*) used body surface area (BSA) to correct the plasma activity in an effort to

Received May 2, 1996; revision accepted Oct. 8, 1996.

For correspondence or reprints contact: M. Donald Blaufox, MD, PhD, Department of Nuclear Medicine, 1695A Eastchester Rd., Bronx, NY 10461.